Plant, Cell & Environment

Plant, Cell and Environment (2014) **37**, 2169–2182 doi: 10.1111/pce.12317

Original Article

Interpreting species-specific variation in tree-ring oxygen isotope ratios among three temperate forest trees

Xin Song[1], Kenneth S. Clark[2] & Brent R. Helliker[1]

[1]*Department of Biology, University of Pennsylvania, Philadelphia, PA 19104, USA and* [2]*Silas Little Experimental Forest, USDA Forest Service, New Lisbon, NJ 08064, USA*

ABSTRACT

Although considerable variation has been documented in tree-ring cellulose oxygen isotope ratios ($\delta^{18}O_{cell}$) among co-occurring species, the underlying causes are unknown. Here, we used a combination of field measurements and modelling to investigate the mechanisms behind variations in late-wood $\delta^{18}O_{cell}$ ($\delta^{18}O_{lc}$) among three co-occurring species (chestnut oak, black oak and pitch pine) in a temperate forest. For two growing seasons, we quantified among-species variation in $\delta^{18}O_{lc}$, as well as several variables that could potentially cause the $\delta^{18}O_{lc}$ variation. Data analysis based on the $\delta^{18}O_{cell}$ model rules out leaf water enrichment ($\Delta^{18}O_{lw}$) and tree-ring formation period (Δt), but highlights source water $\delta^{18}O$ ($\delta^{18}O_{sw}$) as an important driver for the measured difference in $\delta^{18}O_{lc}$ between black and chestnut oak. However, the enriched $\delta^{18}O_{lc}$ in pitch pine relative to the oaks could not be sufficiently explained by consideration of the above three variables only, but rather, we show that differences in the proportion of oxygen exchange during cellulose synthesis (p_{ex}) is most likely a key mechanism. Our demonstration of the relevance of some species-specific features (or lack thereof) to $\delta^{18}O_{cell}$ has important implications for isotope based ecophysiological/paleoclimate studies.

Key-words: among-species variation; p_{ex}; stable oxygen isotope; tree-ring cellulose.

INTRODUCTION

The stable oxygen isotope ratio of tree-ring cellulose ($\delta^{18}O_{cell}$) contains valuable information on an array of environmental and physiological factors that are at work during the period of carbon assimilation and cellulose formation. The rich biotic/abiotic information recorded by $\delta^{18}O_{cell}$ renders $\delta^{18}O_{cell}$, a powerful tool for both paleoclimate and ecophysiological studies. For example, $\delta^{18}O_{cell}$ has been shown to be a good proxy to a number of climatic/physiological factors/events including air temperature (Daux *et al*. 2011), tree canopy temperature (Helliker & Richter 2008; Song *et al*. 2011), precipitation (Brienen *et al*. 2012), relative humidity (RH; Haupt *et al*. 2011) and hurricane activities (Miller *et al*. 2006).

Correspondence: X. Song. Fax: +1 215 898 8780; e-mail: xinsong@sas.upenn.edu; songxbnu@gmail.com

Using $\delta^{18}O_{cell}$ to reconstruct past climates, or tree physiological responses to climate, requires knowledge of both isotopic variation among individual trees within a given species, and isotopic variation among the species that co-occur at the site (McCarroll & Loader 2004; Leavitt 2010). While co-occurring tree species have been documented to exhibit marked variation in their $\delta^{18}O_{cell}$ (Marshall & Monserud 2006; Richter *et al*. 2008; Gebrekirstos *et al*. 2009; Reynolds-Henne *et al*. 2009), the underlying mechanisms behind species-specific affect on $\delta^{18}O_{cell}$ is currently not well understood. Presumably, such a lack of understanding of $\delta^{18}O_{cell}$ variability is largely due to the complex involvement of many environmental and physiological factors in influencing $\delta^{18}O_{cell}$, thereby impeding precise identification of the source(s) of variation.

The mechanistic controls on tree-ring cellulose $\delta^{18}O$ can be partitioned into three primary components: (1) $\delta^{18}O$ of source water ($\delta^{18}O_{sw}$), (2) ^{18}O enrichment of water ($\Delta^{18}O_{mes}$) at the site of triose phosphate and sucrose synthesis (the leaf mesophyll cells) and (3) biochemical fractionation processes that lead to isotopic exchange between organic material and water. These components form the basis of the currently widely used mechanistic model for $\delta^{18}O_{cell}$ (Barbour & Farquhar 2000; Roden *et al*. 2000):

$$\delta^{18}O_{cell} = p_x p_{ex}(\delta^{18}O_{sw} + \varepsilon_o) + (1 - p_x p_{ex})(\Delta^{18}O_{mes} + \delta^{18}O_{sw} + \varepsilon_o) \quad (1)$$

where p_x is the proportion of unenriched xylem water at cellulose synthesis site, p_{ex} is the fraction of oxygen in the cellulose molecule that exchanges with water at the site of cellulose synthesis, ε_o is the biochemical fractionation factor associated with the exchange of oxygen atoms between carbonyl group and the tissue water. In practice, when parameterizing the tree-ring model, two standard assumptions are often made regarding the model parameters, as the following regardless of species: (1) $p_x p_{ex}$ is equal to *ca.* 0.4 due to p_x being close to unity (Barbour 2007) and p_{ex} close to 0.4 (Cernusak *et al*. 2005); and (2) ε_o is equal to *ca.* 27‰ (Sternberg & DeNiro 1983; Cernusak *et al*. 2003). When Eqn 1 is applied to predict $\delta^{18}O_{cell}$, the term $\Delta^{18}O_{mes}$ is usually replaced by $\Delta^{18}O$ of bulk leaf lamina water ($\Delta^{18}O_{lw}$); such a treatment is supported by several lines of experimental and observational evidence obtained from both broad- and needle-leaved species, for which it was demonstrated that

© 2014 John Wiley & Sons Ltd

$\Delta^{18}O_{mes}$ is nearly equivalent to $\Delta^{18}O_{lw}$ (Barbour *et al.* 2000; Cernusak *et al.* 2003; Barnard *et al.* 2007; Gessler *et al.* 2007; Gessler *et al.* 2013).

The tree-ring model (Eqn 1) provides a useful tool for examining potential sources of variation in $\delta^{18}O_{cell}$ among co-occurring species. In the context of this model, and under the above-mentioned two standard assumptions regarding p_{ex} and ε_o, we hypothesize that there are several variables that can potentially exhibit considerable variations among co-occurring species, which in turn may lead to among-species variation in $\delta^{18}O_{cell}$. The first variable is $\delta^{18}O_{sw}$. Variation in $\delta^{18}O_{sw}$ among co-occurring species is commonly observed, primarily because of the among-species difference in rooting depths and therefore the ability to access soil water pools of different isotope compositions (Dawson *et al.* 2002). The second potential source of variation lies in $\Delta^{18}O_{lw}$. An examination of the leaf water enrichment theory (see the Materials and Methods section for more details) indicates that $\Delta^{18}O_{lw}$ variation among co-occurring species is mostly likely to arise, if there is variation in either of the following two controlling factors for $\Delta^{18}O_{lw}$: the Péclet effect (hereafter denoted as f_0; Wang *et al.* 1998; Kahmen *et al.* 2008; Ellsworth *et al.* 2013) and canopy temperature (T_{can}) (Cernusak *et al.* 2007; Brooks & Mitchell 2011). Different species can vary widely in their tree-ring formation periods (Δt). As seasonal amplitudes in environmental factors (e.g. $\delta^{18}O_{sw}$ or relative humidity) or tree functional type (deciduous versus evergreen) can exert controls on $\delta^{18}O_{cell}$, the phenological differences in tree-ring formation are therefore likely to contribute to $\delta^{18}O_{cell}$ differences among species.

In the present study, we investigate the underlying causes of the variability in $\delta^{18}O_{cell}$ among three co-dominant, temperate forest tree species (two broad-leaved deciduous and one needle-leaved evergreen) for two consecutive growing seasons. We performed a rigorous *in situ* examination of the extent of species-specific variation in $\delta^{18}O_{sw}$, $\Delta^{18}O_{lw}$ (including f_0 and T_{can}) and Δt, to determine how these variables contribute to the measured among-species variation in tree-ring $\delta^{18}O_{cell}$. Further, the species-specific data enabled us to fully parameterize the tree-ring model for each species. By comparing the measurement with model predictions, we were able to identify additional sources of $\delta^{18}O_{cell}$ variation that were unaccounted in our initial hypotheses.

MATERIALS AND METHODS

Field measurements

Study site and species

The study was conducted during the growing seasons of 2010 and 2011 at the United States Department of Agriculture Forest Service's Silas Little Experimental Forest, located in Pemberton Township in the Pinelands National Reserve of southern New Jersey, USA (elevation: 35 m, latitude: N 39 °55′, longitude: W 74 °36′). The Pinelands is the largest continuous forested area on the Northeastern coastal region comprising more than 4500 km^2. The climate is cool temperate, with a mean annual temperature of 11.5 °C, and an annual precipitation of 1123 mm. The forest is *ca.* 90 years old, consisting of primarily a mixture of oak and pine species in the overstory. The maximum and mean canopy heights are 18.8 m and *ca.* 8 m, respectively (Skowronski *et al.* 2007; Schäfer 2011). Our study was focused on three dominant species: black oak (*Quercus velutina* Lam.), chestnut oak (*Q. prinus* L.) and pitch pine (*Pinus rigida* Mill.). These three species were ideal for mechanistic study of tree-ring isotope variability for the following two reasons: (1) a pilot field survey that we conducted in 2009 revealed that the three species were all significantly different from each other in $\delta^{18}O_{cell}$ (see Fig. 1); (2) a difficult-to-constrain parameter of the tree-ring model – the Péclet effect of leaf water enrichment – has been intensively studied in all three species in a separate common garden experiment (see Song *et al.* 2013 for details).

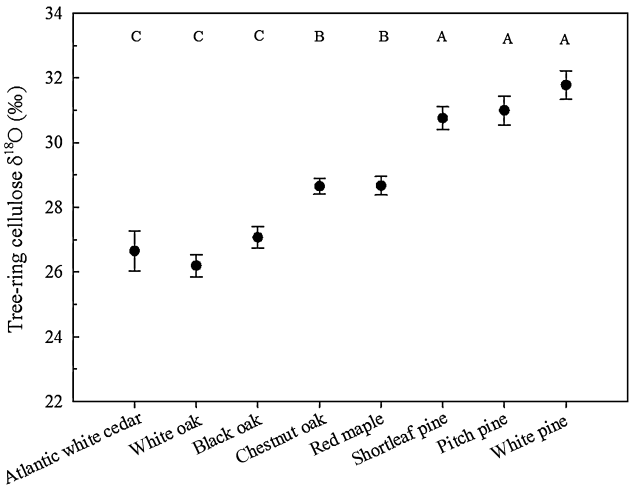

Figure 1. A pilot survey of tree-ring cellulose $\delta^{18}O$ signals from eight tree species co-occurring in the Pine Barrens forest, New Jersey. Tree-ring cellulose $\delta^{18}O$ were analysed from homogenized samples of the most recent 5-year rings (2005–2009). Data shown are mean values ± SE from measurements of six to 10 trees per species. Different letters indicate significant differences between species, as determined by one-way analysis of variance with a Turkey's HSD test.

Meteorological, eddy flux and sap flow measurements

The meteorological and CO_2 eddy flux data used in this study were obtained from 30 min averaged measurements from a 19 m Ameriflux tower installed at the centre of the study area (all data available at http://public.ornl.gov/ameriflux). Air temperature and RH were measured every 10 s using a temperature/humidity probe (HMP45C Vaisala Inc., Woburn, Massachusetts, USA) (Clark *et al.* 2012). The CO_2 exchange between the forest and the atmosphere (NEE) was measured by the eddy-covariance technique as detailed in Clark *et al.* (2010). Gross primary productivity (GPP) was estimated from NEE using a standard flux-partitioning procedure (Reichstein *et al.* 2005; Papale *et al.* 2006).

Measurements of canopy leaf temperature (T_{can}) and radial growth

Trees subject to T_{can} measurements include two black oaks, two chestnut oaks and three pitch pines. For each selected individual, the canopy temperature was measured using an infrared (IR) temperature sensor (model SI-111, Apogee Instruments Inc., Logan, UT, USA). The sensor was mounted either on weather towers or a mast pole, pointing at the canopy of the target tree. The instrument has a 22 ° half angle field of view, and was mounted about 3 to 6 m above the tree canopy, thus monitoring about 8.1 to 18.44 m^2 canopy leaf area. All deployed IR sensors were connected to data loggers (CR1000, Campbell Scientific, Inc., Logan, UT, USA), which scanned each sensor every 60 s, and recorded sample averages every 15 min.

One general complication with IR measurement of canopy temperature is that some non-leaf objects (i.e. tree stems, soil surface etc.) will be unavoidably included in the target area of the IR sensor, causing error in canopy temperature measurement. To minimize exposure of non-leaf materials to the sensor's field of view, we took the following two approaches: (1) we specifically selected tree individuals that had relatively dense canopies to mount the IR sensors; (2) we took effort in adjusting the position and angle of each sensor to ensure the canopy area contained within the sensor's target area was maximal. In a separate field test that was conducted in the growing season of 2009 to evaluate the reliability of the IR sensor method in monitoring canopy leaf temperature, we measured the canopy of a field-grown tree (*Abies balsamea*) with an IR sensor, concomitantly with a network of 20 thermocouples evenly distributed across the canopy. We employed the above-mentioned two approaches in our setup of the IR measurement in this field trial. The results show that throughout the growing season the IR sensor measurements closely matched mean leaf temperatures of the canopy as measured by the thermocouple network (Supporting Information Fig. S1), thereby giving us confidence in the effectiveness of using IR sensors for T_{can} measurement in our current study.

In February 2011, we installed spring-loaded, stainless steel dendrometer bands at the breast height (*ca.* 1.5 m above ground level) on five selected tree individuals for each species. We recorded tree trunk increments from the bands at approximately biweekly intervals, from March to October of 2011.

Plant material and isotope sampling

Samples were collected on approximately biweekly intervals during the growing seasons (May to October) of 2010 and 2011. Between 1200 and 1400 h on each collection day, we used a pole pruner to collect twigs from three randomly chosen trees of each species. The twigs were excised from sun-exposed part of the mid-level tree crown, and were used for collection of leaf and stem samples for isotopic analysis of tissue water. Leaf material, with (for oaks) or without (for pitch pine) the mid-vein removed, and approximately 5–10 cm of lignified stem sections were placed and sealed into separate glass vials. The glass vials were subsequently stored in a freezer until water extraction. On each collection day, the atmospheric water vapour for isotope analysis was collected from the average tree canopy height (*ca.* 8 m above the ground level) within the forest. Water vapour was cryogenically captured by pumping air through dry ice-ethanol cold traps at a flow rate of 500 cm^3 min^{-1} (Helliker *et al.* 2002). Sample collection time usually ranged between 2 and 3 h.

At the end of the 2011 growing season, we sampled tree cores from tree trunks at the breast height using an increment borer of 5 mm diameter (Haglof, Langsele, Sweden). Trees that were radially symmetric were selected for sampling to reduce within-tree variations (Ramesh *et al.* 1985). Two cores were collected from each of a total of six trees per species; one core was used for tree-ring width measurement and the other for isotope analysis.

Tree-ring width measurement and estimates of tree-ring formation periods

Tree cores collected for ring width measurement were sanded to bring up a flat surface with tree-ring boundaries clearly visible. The cores were scanned into images with a flatbed scanner at a resolution of 1600 dpi. From these images, we determined the widths of early-wood, late-wood for tree rings formed in 2010 and 2011, with the aid of the software ImageJ 1.45 (Rasband WS, ImageJ; National Institute of Health, Bethesda, MD, USA).

Measurements taken from the band dendrometers were converted into cumulative radial growth rates (in % of total radial growth of the year), which were then averaged into species-mean values and smoothed out using 'smooth.spline' function in R (Offermann *et al.* 2011). For each species, a tree-ring growth curve (see Fig. 4) was constructed using the smoothed data of that species. By combining the constructed growth curve with the early- and late-wood widths data, we were then able to estimate the periods during which early- and late-wood were formed. As dendrometer data were only available in 2011, we assumed that tree-ring growth phenology remained similar in the year 2010 as that in the measurement year (refer to Supporting Information Fig. S4 for a sensitivity analysis of the validity of this assumption).

Sample processing and mass spectrometry measurements

Tissue water from leaf and stem samples was extracted by cryogenic vacuum distillation (Ehleringer *et al.* 2002). Water samples (0.5 mL) were analysed by equilibration for 48 h in 3 mL Exetainer® vials (Labco limited, Ceredigion, UK) with 10/90 mixture of CO2/He. Four replicates of 100 mL of the headspace, gas was injected into a Gas Chromatography and carried in a helium air stream to a Delta Plus isotope ratio mass spectrometer (Thermo-Finnigan, Bremen, Germany).

Tree cores collected for isotope analysis were cut with a razor blade into early- and late-wood from each of the rings formed in 2010 and 2011. Cellulose was extracted from these

wood samples following the Brendel procedure modified with an addition of 17% NAOH step (wash) to remove hemicellulose (Brendel *et al.* 2000; Gaudinski *et al.* 2005). About 90 to 100 μg cellulose samples were weighed into silver capsules. For isotope analysis, cellulose samples were pyrolyzed at 1100 °C in a Costech Elemental analyser (Costech Analytical Technologies, Valencia, CA, USA). Isotopic composition of the evolved CO gas was determined on a Thermo-Finnigan Delta Plus isotope ratio mass spectrometer, which had a measurement precision of less than 0.23‰ on a standard reference cellulose powder. All cellulose samples were run in triplicate and data were reported on the Standard Mean Ocean Water (SMOW) scale.

Isotope theory and model parameterization

Our investigation of tree-ring isotope variability among species was carried out in the context of the tree-ring mechanistic model, which implicitly assumes that cellulose is derived from photosynthates synthesized during the current growing season. However, it is well-known that, particularly in deciduous tree species, a significant portion of early-wood tree-ring cellulose can originate from remobilized starch synthesized from the previous growing season(s) (Helle & Schleser 2004; Kagawa *et al.* 2006; Offermann *et al.* 2011). Current understanding of the timing, magnitude and fractionation effects associated with starch-storage based cellulose formation is in its infancy, thereby preventing the incorporation of this process into the tree-ring model. As a result of this, our mechanistic investigation was restricted only to late-wood tree-ring cellulose, the isotope signal of which is known to be predominantly controlled by current-year environmental conditions.

The oxygen isotope composition of late-wood tree-ring cellulose ($\delta^{18}O_{lc}$) inherently represents a photosynthesis-weighted average of $\delta^{18}O_{cell}$ signals integrated throughout the late-wood formation period; or

$$\delta^{18}O_{lc} = \frac{\sum_{t_0}^{t_0+\Delta t}(GPP * \delta^{18}O_{cell})}{\sum_{t_0}^{t_0+\Delta t} GPP} \quad (2)$$

where $t = t_0$ and Δt denotes the start and duration of the late-wood formation period respectively, and GPP serves as a proxy to photosynthetic rate. $\delta^{18}O_{cell}$ can be expressed by Eqn 1 as described in the Introduction section.

Using Eqn 1 to calculate $\delta^{18}O_{cell}$ requires that $\Delta^{18}O_{lw}$ be known. $\Delta^{18}O_{lw}$ is theoretically related to f_0 and isotope enrichment of water at the evaporative site ($\Delta^{18}O_{es}$), as the following (Farquhar & Lloyd 1993):

$$\Delta^{18}O_{lw} = f_0 \Delta^{18}O_{es} \quad (3)$$

As aforementioned, the term f_0 specifically refers to the Péclet effect in the current study, but we note that in some previous studies that dealt with the leaf or cellulose isotope models, symbol f or its variants has been used to bear different meanings (Saurer *et al.* 1997; Roden & Ehleringer 1999).

A mathematical expression of the Péclet effect was given by Farquhar & Lloyd (1993), as the following:

$$f_0 = \frac{1 - e^{-\wp}}{\wp} \quad (4)$$

where $\wp = EL/CD$ (denoted as 'Eqn 5'); E is the transpiration rate (mol s^{-1} m^{-2}), L is the scaled effective path length (m), C is the concentration of water (5.55×10^4 mol m^{-3}) and D is the diffusivity of heavy water in water [$D = 119\times10^{-9}$ $exp(-637/(136.15 + T_{can}))$ m^2 s^{-1}] (Cuntz *et al.* 2007).

$\Delta^{18}O_{es}$ in Eqn 3 can be predicted by the steady-state Craig-Gordon model (Craig & Gordon 1965; Flanagan *et al.* 1991):

$$\Delta^{18}O_{es} = \varepsilon^{+} + \varepsilon_k + (\delta^{18}O_{wv} - \delta^{18}O_{sw} - \varepsilon_k)(e_a/e_i) \quad (6)$$

where $\delta^{18}O_{wv}$ denotes isotope composition of atmospheric water vapour; $\varepsilon^{+}$and ε_k are the temperature-dependent equilibrium fractionation factor for the water evaporation and cumulative kinetic fractionation factor of water vapour diffusing out of the leaf, respectively. e_a/e_i represents the ratio of ambient water vapour pressure (e_a) to pressure of water vapour saturated at leaf temperature (e_i). We used canopy leaf temperature (T_{can}, in °C) to parameterize: (1) ε^{+}, according to the equation described by Bottinga & Craig (1969):

$$\varepsilon^{+} = \left[2.644 - 3206/(273.15 + T_{can}) + 1534000/(273.15 + T_{can})^2\right]/1000 \quad (7)$$

and (2) e_i (kPa), through the saturated vapour-pressure and temperature relationship (Buck 1981):

$$e_i = 0.61365 \exp[17.502\, T_{can}/(240.97 + T_{can})] \quad (8)$$

ε_k was calculated as (Farquhar *et al.* 1989; Cappa *et al.* 2003):

$$\varepsilon_k = \left(\frac{32/g_s + 22/g_b}{1/g_s + 1/g_b}\right)\Big/1000 \quad (9)$$

where g_s and g_b are conductance of stomata and boundary layer, respectively.

In practice, to compute $\delta^{18}O_{lc}$ from cellulose synthesized during a given period, we ran Eqn 2 on a time step of 30 min over that period. As no photosynthetic activities would occur in the night, we restricted the model run to daytime hours only (8 to 17 h).

Running Eqn 2 on 30 min time step would require half-hourly values for $\delta^{18}O_{lw}$ (and consequently $\delta^{18}O_{cell}$), which in turn requires half-hourly values for f_0 as one of the inputs. To compute f_0 with Eqns 4 and 5, estimates of both L and E are required. For chestnut oak and pitch pine, we calculated half-hourly L values from E using the empirical L-E relationships determined on these two species in Song *et al.* (2013). It should be noted that Song *et al.* (2013) were unable to obtain a L-E relationship for black oak; we therefore assumed that black oak bears the same L-E relationship as chestnut oak in our calculation of L for black oak. For computing E, we used the following equation: $(1/(1/g_s + 1/g_b))$ $(e_i - e_a)/P$ (denoted as 'Eqn 10'), where P is atmospheric pressure (kPa). g_s was estimated using the Lohammar's function as modified by Oren *et al.* (1999):

$$g_s = g_{ref} - 0.6 \times g_{ref} \times \ln(e_i - e_a) \quad (11)$$

where g_{ref} represents stomatal conductance when ($e_i - e_a$) is 1 kPa. In a recent study that was focused on the same forest site as our current study, Schäfer (2011) was able to make estimations of sap-flux scaled, canopy g_{ref} values for black and chestnut oak under various light regimes in both drought and non-drought conditions. Here, we used the canopy g_{ref} values obtained from that study to parameterize Eqn 11 for the two oaks species (0.12 mol m^{-2} s^{-1} for chestnut oak and 0.15 mol m^{-2} s^{-1} for black oak). As there is no g_{ref} estimation available for pitch pine in the literature, we assumed that canopy g_{ref} was 0.11 mol m^{-2} s^{-1} for pitch pine, based on the estimation made by Oren *et al.* (1999) for a different pine species (*P. sylvestris*) from the temperate biome. Further, for g_b in Eqn 10, we assigned a value of 1.7 mol m^{-2} s^{-1} for black oak, 2 mol m^{-2} s^{-1} for chestnut oak and 2.5 mol m^{-2} s^{-1} for pitch pine, following Song *et al.* (2013) (see Supporting Information Fig. S5 for a sensitivity analysis of the effect on g_b on $\delta^{18}O_{cell}$).

Ideally, for calculating half-hourly $\delta^{18}O_{cell}$ values we would also need half-hourly $\delta^{18}O_{wv}$ values to parameterize Eqn 4. As $\delta^{18}O_{wv}$ measurements at such high resolution were unavailable in our current study, in the calculation we estimated $\delta^{18}O_{wv}$ based on the common assumption that atmospheric water vapour is in isotopic equilibrium with long-term precipitation water. This assumption, as subsequently evaluated using the $\delta^{18}O_{wv}$ data obtained from our biweekly measurements (see the Results section), can be considered to be generally valid in our study site at the seasonal scale.

Statistical analysis

Both $\delta^{18}O_{sw}$ and $\Delta^{18}O_{lw}$ data were analysed separately in each measurement year. Given that tree individuals subjected to leaf/stem water sampling were randomly selected on each sampling day and therefore that they were not always the same individuals across sampling dates, we used a regular (instead of repeated-measures) two-way analysis of variance (ANOVA) to test for differences in $\delta^{18}O_{sw}$ and $\Delta^{18}O_{lw}$ because of the effects of species, sampling dates and their interactions. Whereas for the tree-ring data, we applied a repeated-measures ANOVA to evaluate the effects of species (between-subject factors), wood-type (late- versus early-wood; within-subject factors), year (2010 versus 2011; within-subject factors) and their interactions on tree-ring cellulose $\delta^{18}O$. We considered individual trees as subjects in this analysis.

RESULTS

Climatic conditions and GPP measurements

The growing season of 2010 was drier than 2011. In 2010, growing season precipitation amounted to 368 mm, which was less than half of the precipitation of the 2011 growing season (754 mm; Fig. 2). The growing season mean air temperature and RH were 22.4 °C and 65.1% for 2010, and 21.8 °C and 70.4% for 2011.

Three drought periods were identified throghout the growing seasons of 2010 and 2011: DOY (day of year) 182 to 190, 2010 (Fig. 2, labelled as '1'); DOY 241 to 253, 2010 (Fig. 2, labelled as '2') and DOY 152 to 162, 2011 (Fig. 2, labelled as '3'). These periods were characterized by episodes of high temperautre and low RH, combined with little/no precipitation. Climatic constraints as such led to depression of photosynthesis and consquently reduction in GPP during these drought periods. Such GPP reduction was particularly pronounced in drought period '1' and '2' as was shown in Fig. 2g.

Stem water, atmospheric vapour and leaf water

In both measurement years, stem water $\delta^{18}O$ ($\delta^{18}O_{sw}$) exhibited significant variation among the species ($P < 0.0001$ and $P < 0.0001$ for 2010 and 2011, respectively) and across the sampling days ($P = 0.002$ and $P < 0.0001$ for 2010 and 2011, respectively). A Tukey HSD test revealed that the three species all differed from each other in their $\delta^{18}O_{sw}$ values, with pitch pine having the highest growing season averaged $\delta^{18}O_{sw}$ values (−6.1‰ and −5.9‰ for 2010 and 2011, respectively), black oak the lowest (−8.3‰ and −7.5‰ for 2010 and 2011, respectively) and chestnut oak the intermediate (−7.3‰ and −6.8‰ for 2010 and 2011, respectively). We did not detect significant species × sampling date interaction for $\delta^{18}O_{sw}$ in either year ($P = 0.13$ and 0.19 for 2010 and 2011, respectively). Nevertheless, a visual inspection of the data revealed that drought impact was quite evident in pitch pine $\delta^{18}O_{sw}$, as reflected by the fact that throughout the measurement periods of both years, the three most distinctively enriched $\delta^{18}O_{sw}$ values (−4.5 ± 0.7‰, −4.8 ± 0.6‰, −4.8 ± 0.5‰) in this species were observed in the drought periods '1', '2' and '3' respectively; whereas for both chestnut oak and black oak, distinctions between drought and non-drought $\delta^{18}O_{sw}$ values seem rather small, implying a limited drought impact on $\delta^{18}O_{sw}$ in these two species (Fig. 2a & b).

The measured water vapour $\delta^{18}O$ ($\delta^{18}O_{wv}$) ranged from −18.8 to −13.1‰ and averaged −16.6‰ during the measurement period in 2010; they ranged from −19.9 to −14.3‰ and averaged at −16.8‰ in 2011 (Fig. 3c & d). Under the assumption that at the seasonal scale $^{18}O_{wv}$ is in equilibrium with ^{18}O of amount-weighted annual precipitation water (which is −8‰ at our study site according to Bowen & Revenaugh 2003) at mean growing season temperature, we estimated a growing season mean $\delta^{18}O_{wv}$ value that is *ca.* −17.4‰. This value is close to our measured average $\delta^{18}O_{wv}$ in both 2010 and 2011 (Fig. 3c & d).

For both 2010 and 2011, variation in leaf water isotope enrichment ($\Delta^{18}O_{lw}$) exhibited a significant effect because of sampling date ($P < 0.0001$ for both 2010 and 2011, respectively) and species × sampling date interaction ($P < 0.0001$ for both 2010 and 2011). However, in neither year was a significant species effect observed for $\Delta^{18}O_{lw}$ ($P = 0.45$ and 0.21 for 2010 and 2011, respectively). For each species, we also modelled $\Delta^{18}O_{lw}$ at each sampling time point using the leaf water enrichment model as described by Eqn 3 (see the Materials and Methods section for model parameterization details). For each species/year combination, we averaged the

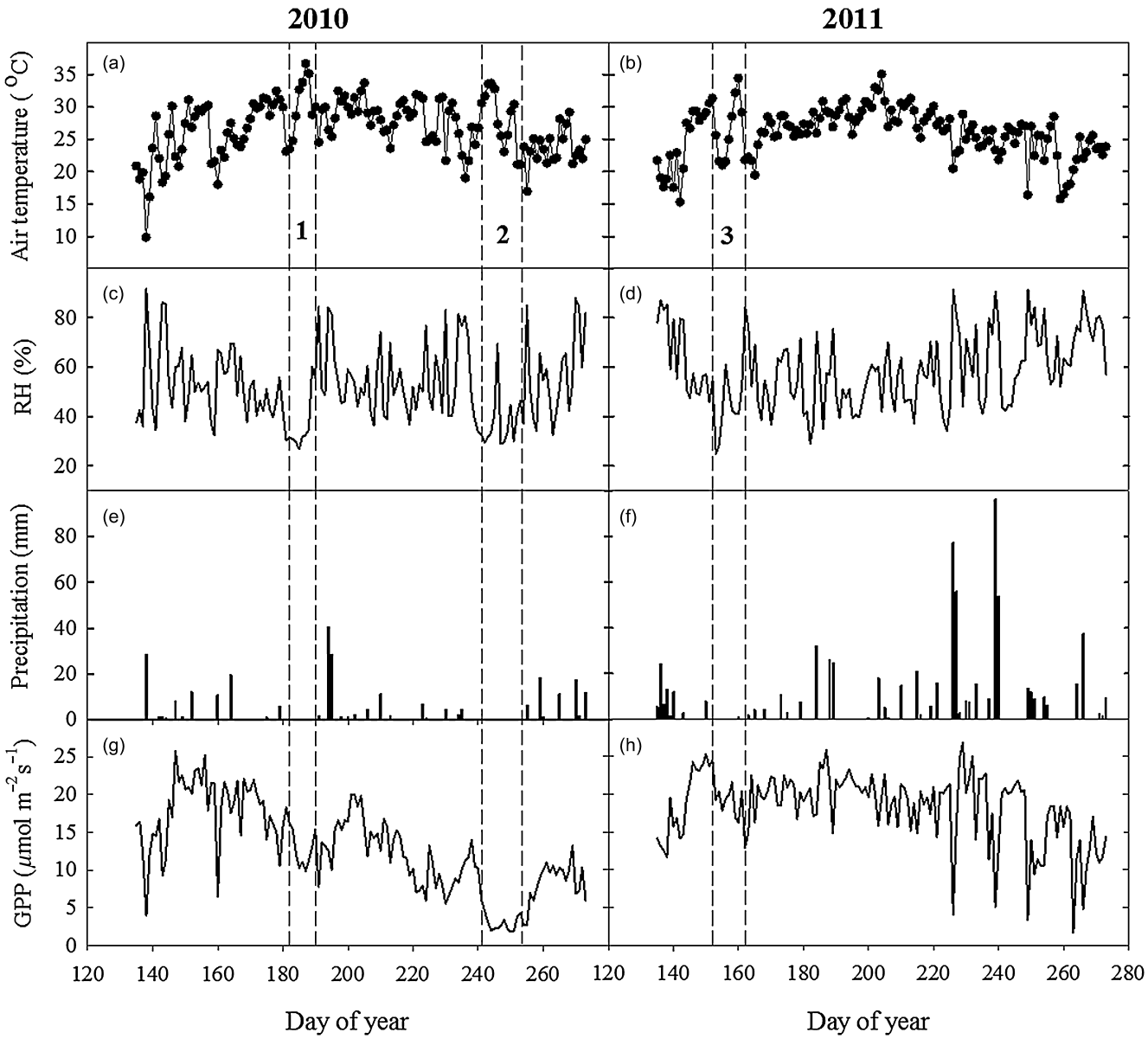

Figure 2. Meterological and flux data during the growing seasons of 2010 and 2011. (a & b) daytime mean air temperature; (c & d) daytime mean relative humidity (RH); (e & f) daily sum of precipitation; (g & h) daytime mean gross primary production (GPP). Daytime period is defined as the period between 8 and 17 h. The three drought periods were denoted by '1', '2' and '3', respectively in the figure.

$\Delta^{18}O_{lw}$ values as modelled at the various sampling time points into a single, growing season value, and we compared this value against the measured $\Delta^{18}O_{lw}$ value as averaged across the same sampling time points. As can be seen from Supporting Information Fig. S2, the model described leaf water enrichment reasonably well across all six species/year combinations, and the correlation analysis between the measured and modelled $\Delta^{18}O_{lw}$ values resulted in $R^2 = 0.836$ ($P = 0.011$).

Wood formation phenology

Figure 4 shows the wood formation periods for each species, as estimated from the dendrometer and tree-ring width data collected in 2011. Phenology of wood formation was rather similar for the two oak species, that is they had identical timing for both wood growth initiation (DOY 98) and cessation (DOY 243), and only differed by 2 d in the timing for early-/late-wood transition (DOY 156 for black oak and 154 for chestnut oak). Pitch pine displayed a much later phenology as compared with the oak species, with its timing for wood growth initiation, cessation and early-/late-wood transition being at DOY 111, 257 and 204, respectively.

GPP-weighted mean T_{can} and f_0

Figure 5a and b show GPP-weighted mean T_{can} (T_{can_GPP}) for each IR sensor measured tree, together with GPP-weighted

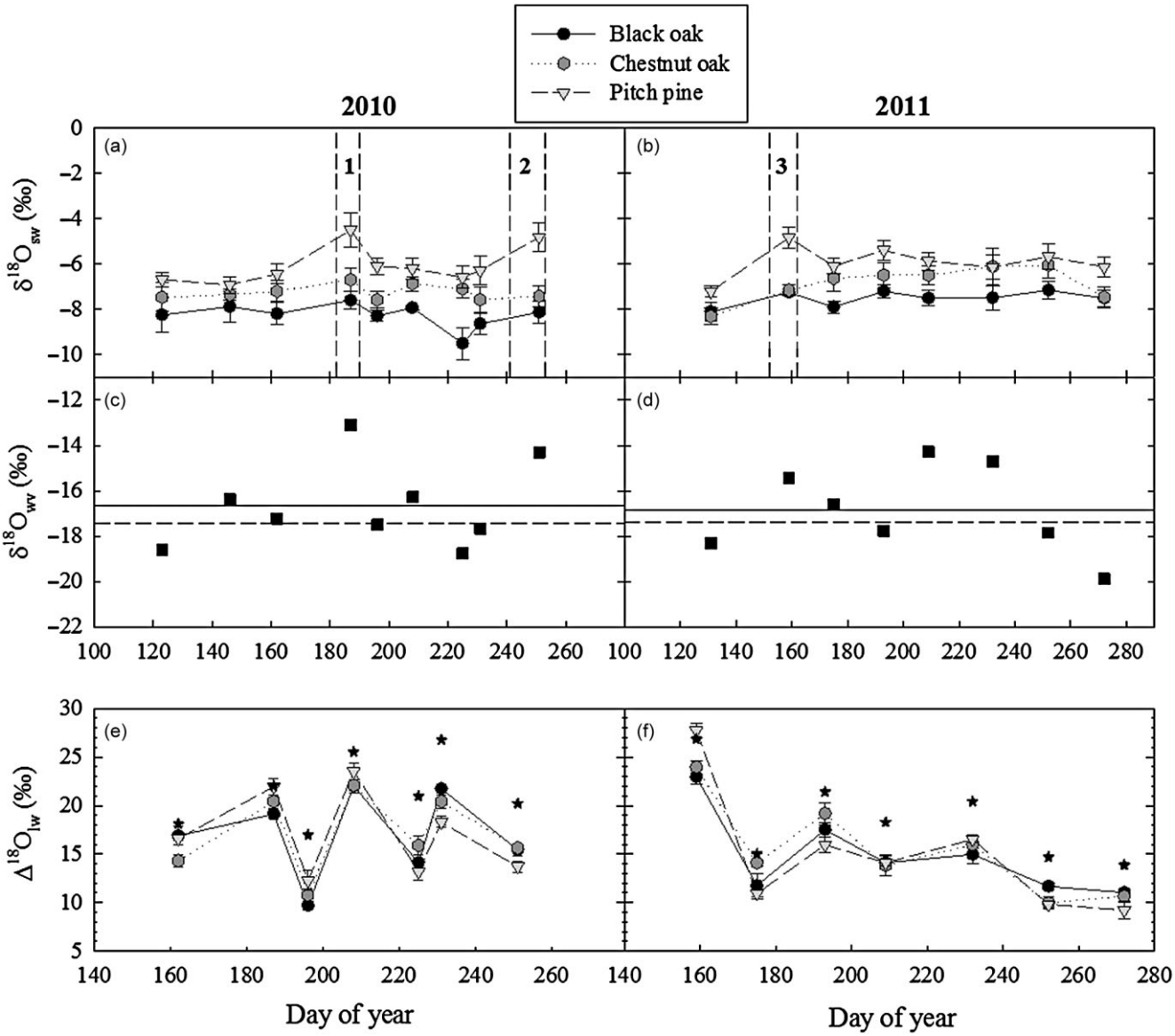

Figure 3. Variations in oxygen isotope compositions in different water pools over the growing seasons of 2010 and 2011. (a & b) oxygen isotope ratios of source water ($\delta^{18}O_{sw}$) in each of the three study species ($n = 3$); the three droughts periods over the measurement periods are denoted by '1', '2' and '3', respectively. (c & d) measured oxygen isotope ratios of atmospheric water vapour ($\delta^{18}O_{wv}$) at the forest canopy height ($n = 1$); the horizontal, solid stand for the measured average $\delta^{18}O_{wv}$ across the measurement periods and the dashed lines for estimated growing season mean $\delta^{18}O_{wv}$ assuming equilibrium with $\delta^{18}O$ of long-term precipitation water. (e & f) oxygen isotope enrichment of leaf water above the source water ($\Delta^{18}O_{lw}$) in each species ($n = 3$); note that $\Delta^{18}O_{lw}$ of pitch pine was calculated by assuming xylem water constitutes 5% of total needle water (Barnard *et al*. 2007). As an example, (e) & (f) also show values for isotope enrichment of water at the evaporative sites ($\Delta^{18}O_{es}$) for chestnut oak (filled stars), which were calculated from Eqn 6 for the leaf water sampling periods at midday.

ambient air temperature (T_{air_GPP}). For the sake of comparison, all values shown in Fig. 5a and b were calculated over the same portion of the growing season (see legend in Fig. 5 for more details). T_{air_GPP} was 27.3 °C in 2010 and 26.9 °C in 2011. In both years, black oak and chestnut oak had very similar T_{can_GPP} values; for example, in 2010, T_{can_GPP} values averaged at 27.2 °C for chestnut oak ($n = 2$), and 27.3 °C for black oak ($n = 2$). Pitch pine had somewhat lower T_{can_GPP} values than the oak species; the average deviations of pitch pine from chestnut oak were −0.4 °C in both 2010 and 2011. In either year, GPP-weighted $T_{can} - T_{air}$ differences were within ±1 °C for all tree individuals measured, suggesting that all three species' canopies were well coupled to the ambient atmospheric conditions.

Shown in Fig. 5c and d are the values for GPP-weighted mean f_0 of each species, calculated over the same portion of the growing season as that for T_{can_GPP}. In 2010, GPP-weighted f_0 values spanned a narrow range from 0.77 for black oak, 0.78 for chestnut oak to 0.81 for pitch pine. Very similar magnitude of among-species variation was also found in 2011 (Fig. 5d).

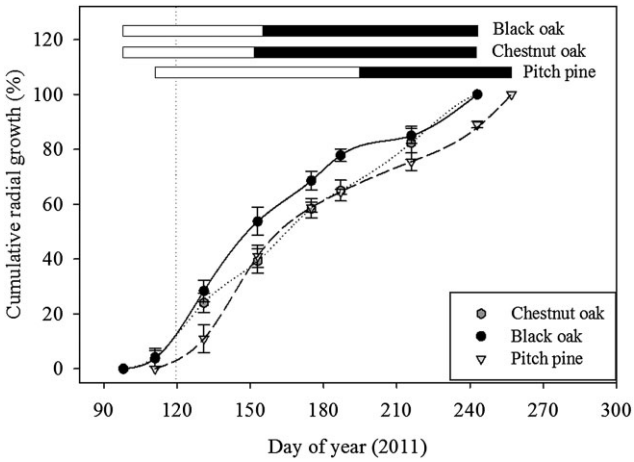

Figure 4. Normalized tree-ring growth curves constructed from the dendrometer measurements on the three tree species ($n = 5$ for each species) during the year 2011. The estimated periods during which early- and late-wood were formed are indicated by horizontal bars, with grey and black bars representing early- and late-wood periods, respectively. The dotted, vertical line delimits the budbreak date for the oak species.

Tree-ring cellulose $\delta^{18}O$

There was significant among-species difference in tree-ring cellulose $\delta^{18}O$ signatures ($P < 0.0001$). Regardless of wood-type, pitch pine had the most enriched $\delta^{18}O$ signal among the three species, whereas black oak had the most depleted signal and chestnut oak was the intermediate (Fig. 6a). This species

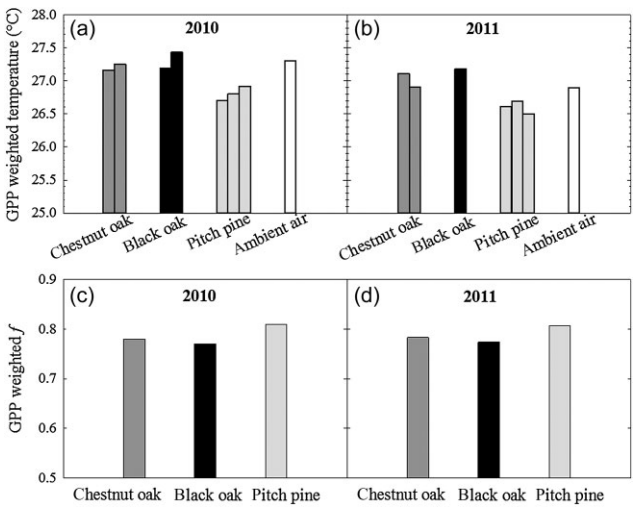

Figure 5. Among-species comparisons of canopy leaf temperatures (a & b) and f_0 (c & d) for 2010 and 2011. (a & b) GPP-weighted mean canopy leaf temperatures for each species, and GPP-weighted mean ambient air tempreatures; (c & d) GPP-weighted mean f_0 for each species. To facilitate comparison, all the values shown in this figure were calculated over the same time period (between DOY 147 and 236, or the measured chestnut oak late-wood formation period). For leaf temperature values in (a) & (b), each bar represents an individual tree.

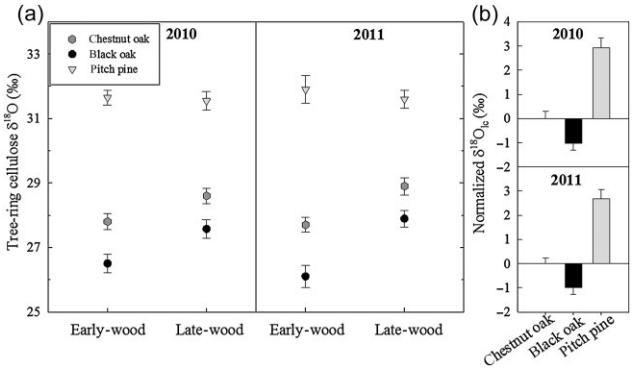

Figure 6. (a) Values for oxygen isotope ratios of early- and late-wood cellulose in tree rings formed in 2010 and 2011; (b) Normalized oxygen isotope ratios of late-wood cellulose ($\delta^{18}O_{lc}$) for each species. To normalize the data, chestnut oak's mean $\delta^{18}O_{lc}$ was subtracted from each tree's $\delta^{18}O_{lc}$ value in a given year. Error bars are standard error of the mean. $n = 6$ for each species.

ranking remained the same for both measurement years and is consistent with the pilot survey results as shown in Fig. 1. We detected a significant interaction between species and wood-type ($P = 0.0033$). Presumably, this is caused by the fact that early-wood isotope signals tended to be considerably more depleted than the corresponding late-wood values for the oak species (see Hill *et al.* 1995 for a similar pattern in *Q. robur*), whereas no such pattern was detected for pitch pine. As our mechanistic investigation was focused on late-wood tree-ring cellulose signal ($\delta^{18}O_{lc}$), to better visualize the species difference, we standardized all $\delta^{18}O_{lc}$ values against the measured $\delta^{18}O_{lc}$ average of chestnut oak in each year. As illustrated in Fig. 6b, when compared against chestnut oak, black oak was more depleted in $\delta^{18}O_{lc}$ by an average of 1.0‰ in both years, whereas pitch pine was more enriched by an average of 2.94 and 2.69‰ in 2010 and 2011, respectively.

Examining the underlying causes for among-species $\delta^{18}O_{lc}$ variation

We used the tree-ring model as a framework to evaluate how the measured among-species variation in each of the four variables ($\delta^{18}O_{sw}$, T_{can}, f_0, Δt) translates to the measured among-species variation in $\delta^{18}O_{lc}$ (see Fig. 7 legend for more details). As the results of our model simulation are similar for both 2010 and 2011, for the sake of brevity, we focus only on the results in 2010.

For the two oak species, $\delta^{18}O_{sw}$ differences led to modelled $\delta^{18}O_{lc}$ differences between black oak and chestnut oak of –0.93‰ (black bar, Fig. 7a), which was very close to the observed $\delta^{18}O_{lc}$ differences (–1.0‰) between these two species. In contrast, the magnitude of the modelled between-species $\delta^{18}O_{lc}$ difference caused by T_{can} or f_0 was small (0.08‰ and –0.11‰, respectively; Fig. 7b & c). When all the three variables ($\delta^{18}O_{sw}$, T_{can} and f_0) were accounted for in the modelling, the modelled $\delta^{18}O_{lc}$ difference between the two oak species remained almost unchanged, regardless of whether or not the small between-species difference in the fourth

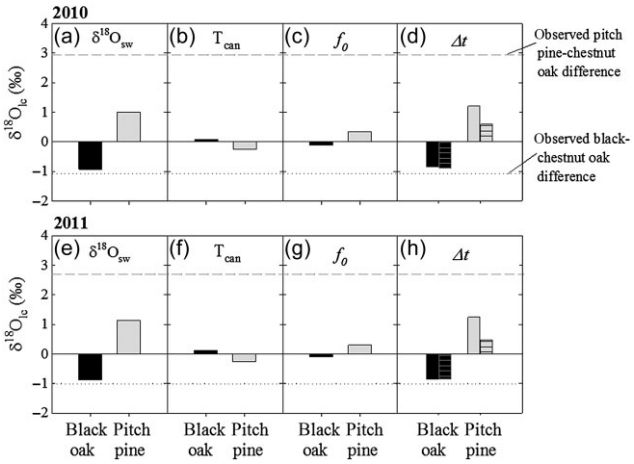

Figure 7. A sensitivity analysis to evaluate how among-species difference in $\delta^{18}O_{sw}$ (b & g), T_{can} (c & h), f_0 (d & i), or wood formation period (e & j) translate into among-species difference in $\delta^{18}O_{lc}$. The modelled default $\delta^{18}O_{lc}$ value of a given year was taken as being the same as the chestnut oak's $\delta^{18}O_{lc}$ value, which was modelled by using what we call the 'default input' values, or the values obtained for chestnut oak in this year to parameterize $\delta^{18}O_{sw}$, T_{can}, f_0 and Δt. (a to c) and (e to f) examine to what extent among-species variation in a target variable would cause $\delta^{18}O_{lc}$ of black oak or pitch pine to differ from the default $\delta^{18}O_{lc}$. For this purpose, in the modelling of $\delta^{18}O_{lc}$ of a species in a given year, the target variable was parameterized with the measured/calculated species-specific values obtained in this year, while all the other variables were held to the default input values. For example, when modelling pitch pine $\delta^{18}O_{lc}$ in (a) and (e), $\delta^{18}O_{sw}$ was parameterized with the collected pitch pine $\delta^{18}O_{sw}$ data while the other model variables (i.e. T_{can}, f_0, and Δt) parameterized with the default input values (or the chestnut oak's values). (d) and (h) specifically illustrate how $\delta^{18}O_{lc}$ in black oak or pitch pine would vary in response to variation in Δt. For this purpose, in modelling $\delta^{18}O_{lc}$ of a given species, $\delta^{18}O_{sw}$, T_{can}, f_0 were all parameterized with species-specific values, while the late-wood formation period either (1) remained to the default period (or the same as that of chestnut), or (2) was parameterized with the species' own wood formation period. In (d) and (h), the modelled $\delta^{18}O_{lc}$ values under scenario (1) and (2) were displayed by the non-hatched and hatched bars, respectively. The data were normalized by subtracting the default $\delta^{18}O_{lc}$ value from the modelled $\delta^{18}O_{lc}$ values in a given year. The dashed and dotted horizontal lines denote the measured average $\delta^{18}O_{lc}$ deviation of black oak and pitch pine from chestnut oak, respectively.

variable – late-wood formation period (or Δt) – was factored into the modelling (as shown by the black and black, hatched bars in Fig. 7d).

The results of our model-measurement comparison show that after accounting for the difference in $\delta^{18}O_{sw}$ between pitch pine and chestnut oak, the modelled $\delta^{18}O_{lc}$ value of pitch pine was only 1‰ more enriched than that of chestnut oak (gray bar, Fig. 7a), and thus inadequate to explain the measured, *ca.* 3‰ enrichment of $\delta^{18}O_{lc}$ in pitch pine relative to chestnut oak. This discrepancy improved only a little if the between-species differences in $\delta^{18}O_{sw}$, T_{can} and f_0 were all taken into account in the modelling (the modelled $\delta^{18}O_{lc}$ difference was 1.2‰, as shown by the gray bar in Fig. 7d), and worsened if the between-species difference in Δt was further controlled as an additional source of variation during the modelling (the modelled $\delta^{18}O_{lc}$ difference was 0.6‰, as shown by the gray, hatched bar in Fig. 7d). Further, our modelling results also show that considering variation in T_{can} or f_0 alone could only cause the pitch pine to deviate from chestnut oak in $\delta^{18}O_{lc}$ to a small degree (–0.25‰ for the case of T_{can}, and 0.34‰ for the case of f_0).

Direct comparison between the modelled and measured $\delta^{18}O_{lc}$ for each species revealed that when all four variables ($\delta^{18}O_{sw}$, T_{can}, f_0 and Δt) were accounted for, the tree-ring mechanistic model gave good prediction of the measured $\delta^{18}O_{lc}$ for both oak species; yet for pitch pine, the model performed poorly in that it severely underestimated the measured $\delta^{18}O_{lc}$ by *ca.* 2.5‰ in both years (Fig. 8a). Such an unsatisfactory model performance in the case of pitch pine prompted us to return to the standard model assumptions regarding $p_x p_{ex} = 0.4$ and $\varepsilon_o = 27$‰; when the model assumptions were altered, either by invoking $p_x p_{ex}$ to be 0.26, or ε_o to be 29.4‰, the severe underestimation of $\delta^{18}O_{lc}$ by the model was largely corrected and consequently we arrived at reasonably good match between the modelled and measured $\delta^{18}O_{lc}$ for pitch pine (Fig. 8b & c).

DISCUSSION

Among-species variation $\delta^{18}O_{sw}$ and its relation to $\delta^{18}O_{lc}$

The three study species showed consistent differences in $\delta^{18}O_{sw}$ throughout the two growing seasons (Fig. 3a), suggesting the presence of interspecific partitioning of water source along the soil profile. The relatively enriched $\delta^{18}O_{sw}$ in pitch pine indicates that it is more reliant upon water in upper soil layers, presumably because of shallower rooting systems. Consequently, pitch pine $\delta^{18}O_{sw}$ signatures were markedly more enriched during the drought periods when the evaporative enrichment of water in the upper soil layers is greater (Zimmermann *et al.* 1967; Hsieh *et al.* 1998; Jackson *et al.* 1999). In contrast, drought effect on $\delta^{18}O_{sw}$ enrichment was not noticeable in either black or chestnut oak, suggesting that these two oak species have limited reliance on water at the upper soil layers. In general, ring-porous oak species show a capacity to utilize water deep in the soil profile, owing to their deep rooting systems (Phillips & Ehleringer 1995; Williams & Ehleringer 2000; Taneda & Sperry 2008). However, in spite of this shared 'deep-rooting' nature, we found that black and chestnut oak still differed from each other in $\delta^{18}O_{sw}$, indicating the potential existence of a further, fine-scale segregation of their functional rooting depths. As is increasingly realized, such a segregation of the so-called 'hydrological niches' as defined by rooting depths constitutes an important mechanism for promoting species coexistence at the local scale (Dawson *et al.* 2002; Moreno-Gutierrez *et al.* 2012).

With regard to $\delta^{18}O_{lc}$, we observed that pitch pine was significantly more enriched than the two oak species (Fig. 6a). This is in line with the results of our pilot survey showing that all pines at our study site were similarly more

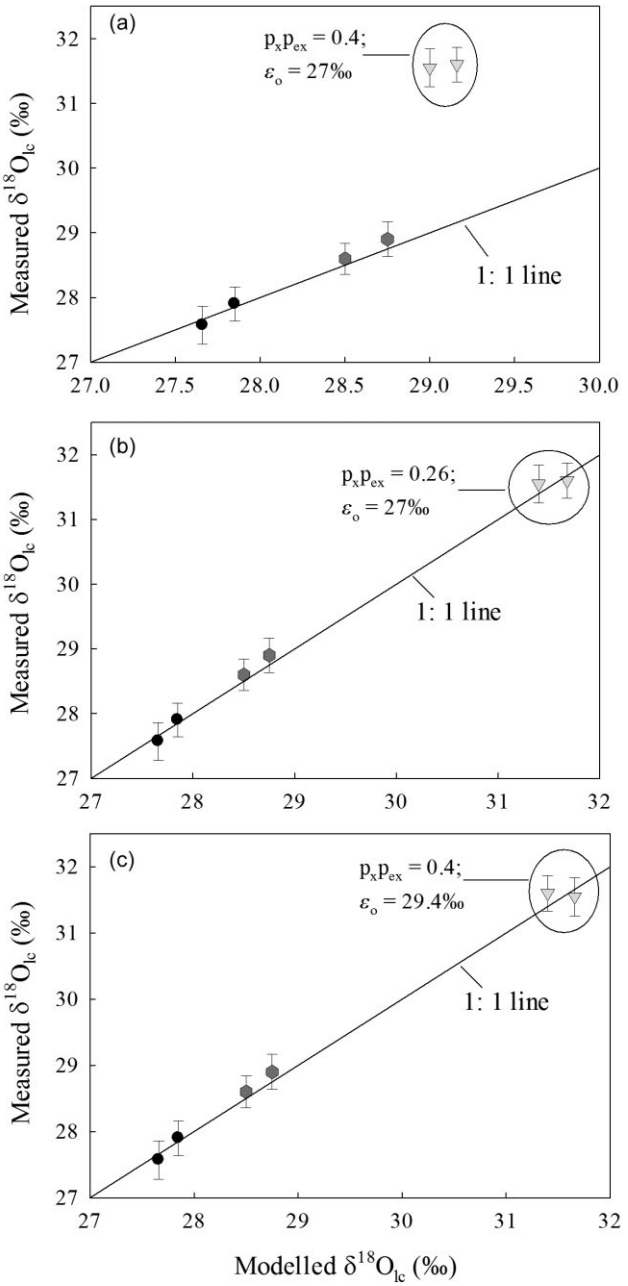

Figure 8. Comparisons of the measured and modelled $\delta^{18}O_{lc}$. In (a), values for p_{ex} and ε_o were taken as being 0.4 and 27‰, respectively in the modelling of $\delta^{18}O_{lc}$ of each species. In (b), model parameterization was the same as in (a) except that a p_{ex} value of 0.26 was used for pitch pine. In (c), model parameterization was the same as in (a) except that ε_o was taken as being 29.4‰ for pitch pine. The 'customized' values of p_{ex} and ε_o for pitch pine in (b) and (c) was chosen because they provided a best-fit for the measured and modelled pitch pine $\delta^{18}O_{lc}$ in each scenario. The symbols are the same as in Fig. 6a.

enriched than broad-leaved deciduous tree species (Fig. 1). Further, our results also agree well with several previous studies in which needle-leaved pine trees were found to be more enriched in tree-ring $\delta^{18}O$ than co-occurring deciduous trees, by *ca.* 2 to 4‰ (Szczepanek *et al.* 2006; Reynolds-Henne *et al.* 2007; Richter *et al.* 2008; Roden & Farquhar 2012). While the more enriched pitch pine $\delta^{18}O_{lc}$ relative to the oaks was qualitatively consistent with the observed $\delta^{18}O_{sw}$ difference between these species, our model analysis showed that $\delta^{18}O_{sw}$ accounted for only a small component of the pine-oak difference (Fig. 7a & e). This contrasts with the two oak species, where the observed $\delta^{18}O_{lc}$ difference was primarily attributed to between-species difference in $\delta^{18}O_{sw}$ (Fig. 7a & e).

Leaf-water enrichment could not explain among-species variation in $\delta^{18}O_{lc}$

Species-level differences in leaf water enrichment of $\delta^{18}O$ have the potential to lead to differences in $\delta^{18}O_{lc}$. Firstly, there are a number of physiological and biophysical factors that can lead to leaf temperature (T_{can}) differences among species, which would impact enrichment directly through e_a/e_i. Secondly, differences in f_0 could impact the isotopic environment in which sucrose was formed and ultimately lead to systematic differences in $\delta^{18}O_{lc}$. We did not, however, observe significant among-species variation in measured $\Delta^{18}O_{lw}$ throughout the growing season in either of the measurement years, suggesting that $\Delta^{18}O_{lw}$ played little role in driving variation in tree-ring isotope signals among species. Additionally, when weighted by GPP over the same portion of a growing season, neither of the two controlling factors of $\Delta^{18}O_{lw}$, – T_{can} and f_0 – exhibited considerable variation among the three species (Fig. 5; see Supporting Information Notes S1 & S2 for more detailed discussion on T_{can} and f_0 variations). Consequently, neither T_{can} or f_0 had any appreciable effect in mediating among-species variation in $\delta^{18}O_{lc}$, as illustrated by the results of our modelling simulation as shown in Fig. 7. Taken together, we can rule out leaf water enrichment as the significant driver for the among-species variation in $\delta^{18}O_{lc}$.

Why are pines more enriched in $\delta^{18}O_{lc}$ than oaks?

The standard assumptions for the cellulose $\delta^{18}O$ model are valid for the oak species, but not for pitch pine. For the two oak species, the tree-ring model predictions based on the standard assumptions of $p_xp_{ex} = 0.4$ and $\varepsilon_o = 27$‰ matched well with observed $\delta^{18}O_{lc}$. In contrast, parameterizing the model with the same assumptions led to an underestimation of $\delta^{18}O_{lc}$ in pitch pine (Fig. 8a). In order for the model to fully account for the measured pitch pine signal, there is a need to alter the model assumptions by either invoking a value of 0.26 for p_xp_{ex} (Fig. 8b) or a value of 29.4‰ for ε_o (Fig. 8c). In the case of $p_xp_{ex} = 0.26$, we can easily infer p_{ex} to be 0.26 if p_x is assumed to be unity. However, previous studies have shown that p_x can be somewhat less than unity; that is p_x was reported to be 0.95 ± 0.03 for trunk tissue of *Eucalyptus* trees in Cernusak *et al.* (2005). In the absence of any actual measurement of p_x in our current study, we choose to be conservative and allow p_x to vary in a considerable range between 0.85

and 1 in our estimates of p_{ex} from the '$p_x p_{ex} = 0.26$' scenario. With such a conservative treatment of p_x uncertainty, we estimate that the p_{ex} value should fall within a range between 0.26 and 0.31 for pitch pine.

The question then arises regarding whether it is p_{ex} or ε_o representing the true mechanism behind the enriched $\delta^{18}O_{lc}$ signal in pitch pine (relative to the oaks). Our measurement design did not allow for direct quantification of p_{ex} or ε_o in pitch pine, which may prevent us from obtaining a definitive answer to this question. However, an examination of literature data leads us to conclude that it is unlikely for pitch pine to have a ε_o value as high as 29.4‰. In two previous studies that involved measurement on the congeneric species *P. sylvestris*, values of ε_o, determined as isotopic difference between needle-leaf water and recent assimilates of leaf, were found to average at *ca.* 27.2‰ (Barnard *et al*. 2007) and *ca.* 25.5‰ (Gessler *et al*. 2013), respectively. Neither of these values is close to the invoked value of 29.4‰ for pitch pine. Recently, Sternberg and Ellsworth (2011) have shown experimentally that ε_o tends to exhibit a negative relationship with plant growth temperature; using the established ε_o and temperature relationship in this study, we infer that growth temperature would need to be *ca.* 11.6 °C for ε_o to reach a value of 29.4‰. Such a low temperature is considerably less than the growing season ambient temperature (*ca.* 22 °C when averaged across the growing season) in our study site; hence considering a temperature effect would also not help justify the possibility of $\varepsilon_o = 29.4$‰ in pitch pine in the current study.

We suggest that invoking a p_{ex} value (i.e. 0.26 to 0.31) different from the commonly assumed value is mostly likely hold the key to fully explaining the observed pitch pine $\delta^{18}O_{lc}$. Theory predicts that p_{ex} is a function of the proportion (denoted as y) of hexose phosphates that undergo triose cycling (or futile cycling) during the synthesis of cellulose from sucrose (Farquhar *et al*. 1998; Barbour & Farquhar 2000). In spite of the evidence that values of p_{ex} tend to average at *ca.* 0.4 across a number of species (Cernusak *et al*. 2005), recent experimental evidence obtained from *Ricinus communis* has revealed the presence of significant variation in p_{ex}, in positive association with the variation in turnover time (τ) of the carbohydrate pool available for cellulose synthesis, potentially as caused by the regulatory effect of τ on y (Song *et al*. 2014). The interdependence between p_{ex} and τ hence renders it possible that broad- and needle-leaved tree species can have different p_{ex} values, for example, if these two tree types inherently differ in τ. Such an inherent difference is plausible considering that broad- and needle-leaved tree species can display substantial difference in several physiological processes, such as carbon allocation pattern and radial growth dynamics (Michelot *et al*. 2012), and that these processes exert great control on carbon turnover rate during cellulose synthesis (Song *et al*. 2014). Furthermore, we note that our estimated p_{ex} range (i.e. 0.26 to 0.31) for pitch pine is in general agreement with the results from the congeneric species *P. sylvestris*, for which p_{ex} ranged from 0.2 to 0.42 (Gessler *et al*. 2009).

Is there oxygen exchange during phloem loading and/or transport?

Recent work by Gessler *et al*. (2013) has shown in several evergreen species that significant organic oxygen exchange with source water can take place during phloem transport of sucrose from the leaf to the site of cellulose synthesis. However, our $\delta^{18}O_{lc}$ data and modelling results do not show clear evidence for the occurrence of phloem related oxygen exchange in the evergreen pitch pine trees. We have demonstrated that under the standard assumption of $p_x p_{ex} = 0.4$ and $\varepsilon_o = 27$‰, the predictions of the cellulose model were less enriched in ^{18}O than observed $\delta^{18}O_{lc}$ in pitch pine (Fig. 8a). If we further allow for a certain degree of oxygen exchange during phloem loading and/or transport (hereafter p_{ex}'), then predicted $\delta^{18}O$ values in pitch pine would be even more depleted than observed $\delta^{18}O_{lc}$. This suggests that oxygen exchange during phloem transport is not plausible in pitch pine. Such a suggestion is in contrast with the observation made in the congeneric species *P. sylvestris*, where p_{ex}' was found to be as high as *ca.* 30% (Gessler *et al*. 2013). Intriguingly, we note that similar inconsistent patterns seem also present for different evergreen *Eucalyptus* species. For example, it was suggested that phloem-related oxygen exchange is a significant process in *Eucalyptus delegatensis* (Gessler *et al*. 2013); yet no evidence was found for this same phenomenon to occur in the congeneric species *E. globulus* (Cernusak *et al*. 2005). These discrepant patterns therefore point to the possibility that oxygen exchange during phloem transport is not a universal phenomenon for all evergreen species. In this context, a better understanding of the role of species characteristics in mediating the transfer of $\delta^{18}O$ signal from leaf to the cellulose synthesis site is clearly needed.

CONCLUSIONS

Our study demonstrates that the measured, *ca.* 1‰ differences in $\delta^{18}O_{lc}$ between black and chestnut oak were primarily driven by $\delta^{18}O_{sw}$, but not by variables (T_{can} and f_0) operating at the leaf water level (or $\Delta^{18}O_{lw}$ per se), nor by Δt that is operational at the temporal scale. Regarding the substantially more enriched $\delta^{18}O_{lc}$ signals in pitch pine relative to the oaks, we show that none of the our initially hypothesized variables ($\delta^{18}O_{sw}$, $\Delta^{18}O_{lw}$ and Δt) could account for such a pattern. Rather, the model-measurement comparison that we performed suggests that invoking a p_{ex} value that is much lower than the commonly assumed value of 0.4 is mostly likely necessary to adequately explain the observed $\delta^{18}O_{lc}$ difference between pitch pine and the oak species.

As such, our study provides insights into several aspects of the mechanistic controls (or lack thereof) on tree-ring isotope signals in a species-specific context; such insights are much needed for an enhancement in our working ability to appropriately parameterize the model in various contexts, and consequently for an improvement in our confidence in applying the model to different tree species in future ecophysiological/environmental studies.

ACKNOWLEDGMENTS

We would like to thank Erin Wiley and Dustin Bronson for help in the field, David Vann for isotope analysis and Nicholas Distefano for water extraction. We thank Margaret Barbour, Graham Farquhar, Ansgar Kahmen and two anonymous reviewers for their constructive comments on an early version of the manuscript. This work was supported by the National Science Foundation under award number IOS-0950998 (to B.R.H. and X.S.).

REFERENCES

Barbour M.M. (2007) Stable oxygen isotope composition of plant tissue: a review. *Functional Plant Biology* **34,** 83–94.

Barbour M.M. & Farquhar G.D. (2000) Relative humidity- and ABA-induced variation in carbon and oxygen isotope ratios of cotton leaves. *Plant, Cell & Environment* **23,** 473–485.

Barbour M.M., Schurr U., Henry B.K., Wong S.C. & Farquhar G.D. (2000) Variation in the oxygen isotope ratio of phloem sap sucrose from castor bean. Evidence in support of the Péclet effect. *Plant Physiology* **123,** 671–679.

Barnard R.L., Salmon Y., Kodama N., Sorgel K., Holst J., Rennenberg H., Gessler A. & Buchmann N. (2007) Evaporative enrichment and time lags between $d^{18}O$ of leaf water and organic pools in a pine stand. *Plant, Cell & Environment* **30,** 539–550.

Bottinga Y. & Craig H. (1969) Oxygen isotope fractionation between CO_2 and water and isotopic composition of marine atmospheric CO_2. *Earth and Planetary Science Letters* **5,** 285–295.

Bowen G.J. & Revenaugh J. (2003) Interpolating the isotopic composition of modern meteoric precipitation. *Water Resources Research* **39,** 1299–1311.

Brendel O., Iannetta P.P.M. & Stewart D. (2000) A rapid and simple method to isolate pure alpha-cellulose. *Phytochemical Analysis* **11,** 7–10.

Brienen R.J.W., Helle G., Pons T.L., Guyot J.L. & Gloor M. (2012) Oxygen isotopes in tree rings are a good proxy for Amazon precipitation and El Nino-Southern Oscillation variability. *Proceedings of the National Academy of Sciences of the United States of America* **109,** 16957–16962.

Brooks J.R. & Mitchell A.K. (2011) Interpreting tree responses to thinning and fertilization using tree-ring stable isotope. *New Phytologist* **190,** 770–782.

Buck A.L. (1981) New equations for computing vapor pressure and enhancement factor. *Journal of Applied Meteorology* **20,** 1527–1532.

Cappa C.D., Hendricks M.B., DePaolo D.J. & Cohen R.C. (2003) Isotopic fractionation of water during evaporation. *Journal of Geophysical Research* **108,** 4525–4534.

Cernusak L.A., Wong S.C. & Farquhar G.D. (2003) Oxygen isotope composition of phloem sap in relation to leaf water in *Ricinus communis*. *Functional Plant Biology* **30,** 1059–1070.

Cernusak L.A., Farquhar G.D. & Pate J.S. (2005) Environmental and physiological controls over oxygen and carbon isotope composition of Tasmanian blue gum, *Eucalyptus globulus*. *Tree Physiology* **25,** 129–146.

Cernusak L.A., Winter K., Aranda J., Turner B.L. & Marshall J.D. (2007) Transpiration efficiency of a tropical pioneer tree (Ficus insipida) in relation to soil fertility. *Journal of Experimental Botany* **58,** 3549–3566.

Clark K.L., Skowronski N. & Hom J. (2010) Invasive insects impact forest carbon dynamics. *Global Change Biology* **16,** 88–101.

Clark K.L., Skowronski N., Gallagher M., Renninger H. & Schäfer K. (2012) Effects of invasive insects and fire on forest energy exchange and evapotranspiration in the New Jersey Pinelands. *Agricultural and Forest Meteorology* **166–167,** 50–61.

Craig H. & Gordon L.I. (1965) Deuterium and oxygen-18 variations in the ocean and the marine atmosphere. In *Proceeding of the Conference on Stable Isotopes in Oceanographic Studies and Palaeotemperatures* (ed. T. Tongiorgi), pp. 9–130. Lab. Geologia Nucleare, Spoleto, Italy.

Cuntz M., Ogee J., Farquhar G.D., Peylin P. & Cernusak L.A. (2007) Modelling advection and diffusion of water isotopologues in leaves. *Plant, Cell & Environment* **30,** 892–909.

Daux V., Edouard J.L., Masson-Delmotte V., Stievenard M., Hoffmann G., Pierre M., . . . Guibal F. (2011) Can climate variations be inferred from tree-ring parameters and stable isotopes from *Larix decidua*? Juvenile effects, budmoth outbreaks, and divergence issue. *Earth and Planetary Science Letters* **309,** 221–233.

Dawson T.E., Mambelli S., Plamboeck A.H., Templer P.H. & Tu K.P. (2002) Stable isotopes in plant ecology. *Annual Review of Ecology and Systematics* **33,** 507–559.

Ehleringer J.R., Bowling D.R., Flanagan L.B., Fessenden J., Helliker B., Martinelli L.A. & Ometto J.P. (2002) Stable isotopes and carbon cycle processes in forests and grasslands. *Plant Biology* **4,** 181–189.

Ellsworth P.V., Ellsworth P.Z., Anderson W.T. & Sternberg L.S.L. (2013) The role of effective leaf mixing length in the relationship between the delta O-18 of stem cellulose and source water across a salinity gradient. *Plant, Cell & Environment* **36,** 138–148.

Farquhar G.D. & Lloyd J. (1993) Carbon and oxygen isotope effects in the exchange of carbon dioxide between terrestrial plants and the atmosphere. In *Stable Isotopes and Plant Carbon–Water Relations* (eds J.R. Ehleringer, A.E. Hall & G.D. Farquhar), pp. 47–70. Academic Press, San Diego, CA, USA.

Farquhar G.D., Hubick K.T., Condon A.G. & Richards R.A. (1989) Carbon isotope fractionation and plant water-use efficiency. In *Stable Isotopes in Ecological Research* (eds P.W. Rundel, J.R. Ehleringer & K.A. Nagy), pp. 21–46. Springer, New York, NY, USA.

Farquhar G.D., Barbour M.M. & Henry B.K. (1998) Interpretation of oxygen isotope composition of leaf material. In *Stable Isotopes: Integration of Biological, Ecological and Geochemical Processes* (ed. H. Griffiths), pp. 27–62. Bios Scientific Publishers, Oxford, UK.

Flanagan L.B., Comstock J.P. & Ehleringer J.R. (1991) Comparison of modeled and observed environmental-influences on the stable oxygen and hydrogen isotope composition of leaf water in *Phaseolus vulgaris l. Plant Physiology* **96,** 588–596.

Gaudinski J.B., Dawson T.E., Quideau S., Schuur E.A.G., Roden J.S., Trumbore S.E., . . . Wasylishen R.E. (2005) Comparative analysis of cellulose preparation techniques for use with C-13, C-14, and O-18 isotopic measurements. *Analytical Chemistry* **77,** 7212–7224.

Gebrekirstos A., Worbes M., Teketay D., Fetene M. & Mitlohner R. (2009) Stable isotope ratios in tree rings of co-occurring species from semi-arid tropics in Africa: patterns and climatic signals. *Global and Planetary Change* **66,** 253–260.

Gessler A., Peuke A.D., Keitel C. & Farquhar G.D. (2007) Oxygen isotope enrichment of organic matter in *Ricinus communis* during the diel course and as affected by assimilate transport. *New Phytologist* **174,** 600–613.

Gessler A., Brandes E., Buchmann N. , Helle G., Rennenberg H. & Barnard R. (2009) Tracing carbon and oxygen isotope signals from newly assimilated sugars in the leaves to the tree-ring archive. *Plant, Cell and Environment* **32,** 780–795.

Gessler A., Brandes E., Keitel C., Boda S., Kayler Z.E., Granier A., Barbour M., Farquhar G.D. & Treydte K. (2013) The oxygen isotope enrichment of leaf-exported assimilates – does it always reflect lamina leaf water enrichment? *New Phytologist* **200,** 144–157.

Haupt M., Weigl M., Grabner M. & Boettger T. (2011) A 400-year reconstruction of July relative air humidity for the Vienna region (eastern Austria) based on carbon and oxygen stable isotope ratios in tree-ring latewood cellulose of oaks (*Quercus petraea Matt. Liebl*). *Climatic Change* **105,** 243–262.

Helle G. & Schleser G.H. (2004) Beyond CO2-fixation by Rubisco – an interpretation of C-13/C-12 variations in tree rings from novel intra-seasonal studies on broad-leaf trees. *Plant, Cell & Environment* **27,** 367–380.

Helliker B.R. & Richter S.L. (2008) Subtropical to boreal convergence of tree-leaf temperatures. *Nature* **454,** 511–514.

Helliker B.R., Roden J.S., Cook C. & Ehleringer J.R. (2002) A rapid and precise method for sampling and determining the oxygen isotope ratio of atmospheric water vapor. *Rapid Communications in Mass Spectrometry* **16,** 929–932.

Hill S.A., Waterhouse J.S., Field E.M., Switsur V.R. & Aprees T. (1995) Rapid recycling of triose phosphates in oak stem tissue. *Plant, Cell & Environment* **18,** 931–936.

Hsieh J.C.C., Chadwick O.A., Kelly E.F. & Savin S.M. (1998) Oxygen isotopic composition of soil water: quantifying evaporation and transpiration. *Geoderma* **82,** 269–293.

Jackson P.C., Meinzer F.C., Bustamante M., Goldstein G., Franco A., Rundel P.W., . . . Causin F. (1999) Partitioning of soil water among tree species in a Brazilian Cerrado ecosystem. *Tree Physiology* **19,** 717–724.

Kagawa A., Sugimoto A. & Maximov T.C. (2006) (CO2)-C-13 pulse-labelling of photoassimilates reveals carbon allocation within and between tree rings. *Plant, Cell & Environment* **29,** 1571–1584.

Kahmen A., Simonin K., Tu K.P., Merchant A., Callister A., Siegwolf R., . . . Arndt S.K. (2008) Effects of environmental parameters, leaf physiological properties and leaf water relations on leaf water delta O-18 enrichment in different *Eucalyptus* species. *Plant, Cell & Environment* **31,** 738–751.

Leavitt S.W. (2010) Tree-ring C-H-O isotope variability and sampling. *Science of the Total Environment* **408,** 5244–5253.

McCarroll D. & Loader N.J. (2004) Stable isotopes in tree rings. *Quartenary Science Reviews* **23,** 771–801.

Marshall J.D. & Monserud R.A. (2006) Co-occurring species differ in tree-ring delta O-18 trends. *Tree Physiology* **26,** 1055–1066.

Michelot A., Simard S., Rathgeber C., Dufrene E. & Damesin C. (2012) Comparing the intra-annual wood formation of three European species (*Fagus sylvatica, Quercus petraea and Pinus sylvestris*) as related to leaf phenology and non-structural carbohydrate dynamics. *Tree Physiology* **32,** 1033–1045.

Miller D.L., Mora C.I., Grissino-Mayer H.D., Mock C.J., Uhle M.E. & Sharp Z. (2006) Tree-ring isotope records of tropical cyclone activity. *Proceedings of the National Academy of Sciences of the United States of America* **103,** 14294–14297.

Moreno-Gutierrez C., Dawson T.E., Nicolas E. & Querejeta J.I. (2012) Isotopes reveal contrasting water use strategies among coexisting plant species in a Mediterranean ecosystem. *New Phytologist* **196,** 489–496.

Offermann C., Ferrio J.P., Holst J., Grote R., Siegwolf R., Kayler Z. & Gessler A. (2011) The long way down–are carbon and oxygen isotope signals in the tree ring uncoupled from canopy physiological processes? *Tree Physiology* **31,** 1088–1102.

Oren R., Sperry J.S., Katul G.G., Pataki D.E., Ewers B.E., Phillips N. & Schäfer K.V.R. (1999) Survey and synthesis of intra- and interspecific variation in stomatal sensitivity to vapour pressure deficit. *Plant, Cell & Environment* **22,** 1515–1526.

Papale D., Reichstein M., Aubinet M., Canfora E., Bernhofer C., Kutsch W., . . . Yakir D. (2006) Towards a standardized processing of net ecosystem exchange measured with eddy covariance technique: algorithms and uncertainty estimation. *Biogeosciences* **3,** 571–583.

Phillips S.L. & Ehleringer J.R. (1995) Limited uptake of summer precipitation by bigtooth maple (*Acer grandidentatum Nutt*) and Gambels oak (*Quercus gambelii Nutt*). *Trees-Structure and Function* **9,** 214–219.

Ramesh R., Bhattacharya S.K. & Gopalan K. (1985) Dendroclimatological implications of isotope coherence in trees from Kashmir Valley, India. *Nature* **317,** 802–804.

Reichstein M., Falge E., Baldocchi D., Papale D., Aubinet M., Berbigier P., . . . Valentini R. (2005) On the separation of net ecosystem exchange into assimilation and ecosystem respiration: review and improved algorithm. *Global Change Biology* **11,** 1424–1439.

Reynolds-Henne C.E., Siegwolf R.T.W., Treydte K.S., Esper J., Henne S. & Saurer M. (2007) Temporal stability of climate-isotope relationships in tree rings of oak and pine (Ticino, Switzerland). *Global Biogeochemical Cycles* **21,** 1–12.

Reynolds-Henne C.E., Saurer M. & Siegwolf R.T.W. (2009) Temperature versus species specific influences on the stable oxygen isotope ratio of tree rings. *Trees-Structure and Function* **23,** 801–811.

Richter S.L., Johnson A.H., Dranoff M.M., LePage B.A. & Williams C.J. (2008) Oxygen isotope ratios in fossil wood cellulose: isotopic composition of eocene- to holocene-aged cellulose. *Geochimica et Cosmochimica Acta* **72,** 2744–2753.

Roden J. S. & Ehleringer J. R. (1999) Observations of hydrogen and oxygen isotopes in leaf water confirm the Craig-Gordon model under wide-ranging environmental conditions. *Plant Physiology* **120,** 1165–1173.

Roden J.S., Lin G.G. & Ehleringer J.R. (2000) A mechanistic model for interpretation of hydrogen and oxygen isotope ratios in tree-ring cellulose. *Geochimica et Cosmochimica Acta* **64,** 21–35.

Roden J.S. & Farquhar G.D. (2012) A controlled test of the dual-isotope approach for the interpretation of stable carbon and oxygen isotope ratio variation in tree rings. *Tree Physiology* **32,** 490–503.

Saurer M., Aellen K. & Siegwolf R.T.W. (1997) Correlating $\delta^{13}C$ and $\delta^{18}O$ in cellulose of trees. *Plant, Cell & Environment* **20,** 1543–1550.

Schäfer K.V.R. (2011) Canopy stomatal conductance following drought, disturbance, and death in an upland oak/pine forest of the New Jersey Pine Barrens, USA. *Frontiers in Plant Science* **2,** 1–7.

Skowronski N., Clark K., Nelson R., Hom J. & Patterson M. (2007) Remotely sensed measurements of forest structure and fuel loads in the Pinelands of New Jersey. *Remote Sensing of Environment* **108,** 123–129.

Song X., Barbour M.M., Saurer M. & Helliker B.R. (2011) Examining the large-scale convergence of photosynthesis-weighted tree-leaf temperatures through stable oxygen isotope analysis of multiple datasets. *New Phytologist* **192,** 912–924.

Song X., Barbour M.M., Farquhar G.D., Vann D.R. & Helliker B.R. (2013) Transpiration rate relates to within- and across-species variations in effective path length in a leaf water model of oxygen isotope enrichment. *Plant, Cell & Environment* **36,** 1338–1351.

Song X., Farquhar G.D., Gessler A. & Barbour M.M. (2014) Turnover time of the non-structural carbohydrate pool influences $d^{18}O$ of leaf cellulose. *Plant, Cell & Environment* doi: 10.1111/pce.12309.

Szczepanek M., Pazdur A., Pawelczyk S., Bottger T., Haupt M., Halas S., . . . Szychowska-Krapiec E. (2006) Hydrogen, carbon and oxygen isotopes in pine and oak tree rings from Southern Poland as climatic indicators in years 1900–2003. *Geochronometria* **25,** 67–76.

Sternberg L. & Deniro M.J. (1983) Bio-geochemical implications of the isotopic equilibrium fractionation factor between oxygen atoms of acetone and water. *Geochimica et Cosmochimica Acta* **47,** 2271–2274.

Sternberg L. & Ellsworth P.V. (2011) Divergent biochemical fractionation, not convergent temperature, explains cellulose oxygen isotope enrichment across latitudes. *PLoS ONE* **6**(11): e28040.

Taneda H. & Sperry J.S. (2008) A case-study of water transport in co-occurring ring- versus diffuse-porous trees: contrasts in water-status, conducting capacity, cavitation and vessel refilling. *Tree Physiology* **28,** 1641–1651.

Wang X.F., Yakir D. & Avishai M. (1998) Non-climatic variations in the oxygen isotopic compositions of plants. *Global Change Biology* **4,** 835–849.

Williams D.G. & Ehleringer J.R. (2000) Intra- and interspecific variation for summer precipitation use in pinyon-juniper woodlands. *Ecological Monographs* **70,** 517–537.

Zimmermann U., Ehhalt D. & Munnich K.O. (1967) Soil-water movement and evaporation: changes in isotopic composition of the water. In *Proceedings of the Symposium on Isotopes in Hydrology* (ed. M. Knippner), pp. 567–584. IAEA, Vienna, Austria.

Received 6 March 2013; received in revised form 24 February 2014; accepted for publication 25 February 2014

SUPPORTING INFORMATION

Additional Supporting Information may be found in the online version of this article at the publisher's web-site:

Figure S1. Canopy temperatures as measured by thermocouples versus by an IR sensor. A 10-m tall balsam fir (*Abies balsamea*) tree grown in the Whiteface mountain forest, New York was chosen for such measurement. Twenty thermocouples were placed evenly across the tree canopy to measure the average canopy temperatures (*y*-axis data), which were compared against canopy temperatures measured by an IR sensor (*x*-axis data). The measurements were made continuously from June to September 2008; however, only daytime temperature data are shown in the figure.

Figure S2. Comparisons of the measured and modelled, sampling-period averaged $\Delta^{18}O_{lw}$ values across the six species/year combinations. The symbols are the same as in Fig. 6a.

Figure S3. The species-specific f_0-E relationships as shown in this figure were deduced based on Eqns 4 and 5 using the species-specific *L-E* relationships as determined by Song *et al*. (2013). Leaf temperature was assumed at 27 °C for calculating diffusivity factor *D*.

Figure S4. Results for a sensitivity analysis testing the effect of variations in late-wood formation period (<ι>Δt</ι>) on $\delta^{18}O_{lc}$ for the year 2010. For each species, the default input values for the late-wood starting and ending days were the

same as the values empirically determined in 2011. In (a), the late-wood ending day was held to each species' default value while the starting day was independently varied by ± 5 and ± 10 d. In (b), the late-wood starting day was held to each species' default value while the ending day was independently varied by ± 5 and ± 10 d.

Figure S5. Results for a sensitivity analysis testing the effect of variations in boundary conductance (g_b) on $\delta^{18}O_{lc}$ in the years 2010 (a) and 2011 (b). Default input values of g_b were 2 mol m^{-2} s^{-1} for chestnut oak, 1.7 mol m^{-2} s^{-1} for black oak and 2.5 mol m^{-2} s^{-1} for pitch pine. For each species/year combination, values for g_b were independently varied by ± 50% and ± 100% while all the other variables of the tree-ring model remained unchanged.

Note S1. Among-species variation in T_{can}.

Note S2. Among-species variation in f_0.